

Title	Second-order data obtained from differential pulse voltammetry: Determination of tryptophan at a gold nanoparticles decorated multiwalled carbon nanotube modified glassy carbon electrode
Authors	Kooshki, Mojtaba; Abdollahi, Hamid; Bozorgzadeh, Somayyeh; Haghghi, Behzad
Publication date	2011-08-05
Original Citation	Kooshki, M., Abdollahi, H., Bozorgzadeh, S. and Haghghi, B. (2011) 'Second-order data obtained from differential pulse voltammetry: Determination of tryptophan at a gold nanoparticles decorated multiwalled carbon nanotube modified glassy carbon electrode', <i>Electrochimica Acta</i> , 56 (24), pp. 8618-8624. doi: 10.1016/j.electacta.2011.07.049
Type of publication	Article (peer-reviewed)
Link to publisher's version	<a href="https://doi.org/10.1016/j.electacta.2011.07.049">https://doi.org/10.1016/j.electacta.2011.07.049</a> - <a href="https://doi.org/10.1016/j.electacta.2011.07.049">10.1016/j.electacta.2011.07.049</a>
Rights	© 2021 Elsevier Ltd. This manuscript version is made available under the CC-BY-NC-ND 4.0 license <a href="https://creativecommons.org/licenses/by-nc-nd/4.0/">https://creativecommons.org/licenses/by-nc-nd/4.0/</a> - <a href="https://creativecommons.org/licenses/by-nc-nd/4.0/">https://creativecommons.org/licenses/by-nc-nd/4.0/</a>
Download date	2024-07-14 08:22:37
Item downloaded from	<a href="https://hdl.handle.net/10468/13518">https://hdl.handle.net/10468/13518</a>



# UCC

**University College Cork, Ireland**  
Coláiste na hOllscoile Corcaigh

## Accepted Manuscript

Title: Second-order data obtained from differential pulse voltammetry: determination of tryptophan at a gold nanoparticles decorated multiwalled carbon nanotube modified glassy carbon electrode

Authors: Mojtaba Kooshki, Hamid Abdollahi, Somayyeh Bozorgzadeh, Behzad Haghighi

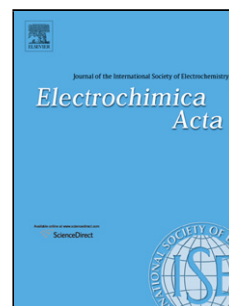
PII: S0013-4686(11)01062-0  
DOI: doi:10.1016/j.electacta.2011.07.049  
Reference: EA 17433

To appear in: *Electrochimica Acta*

Received date: 14-5-2011  
Revised date: 14-7-2011  
Accepted date: 14-7-2011

Please cite this article as: M. Kooshki, H. Abdollahi, S. Bozorgzadeh, B. Haghighi, Second-order data obtained from differential pulse voltammetry: determination of tryptophan at a gold nanoparticles decorated multiwalled carbon nanotube modified glassy carbon electrode, *Electrochimica Acta* (2010), doi:10.1016/j.electacta.2011.07.049

This is a PDF file of an unedited manuscript that has been accepted for publication. As a service to our customers we are providing this early version of the manuscript. The manuscript will undergo copyediting, typesetting, and review of the resulting proof before it is published in its final form. Please note that during the production process errors may be discovered which could affect the content, and all legal disclaimers that apply to the journal pertain.



1  
2  
3  
4 **Second-order data obtained from differential pulse voltammetry: determination of**  
5  
6 **tryptophan at a gold nanoparticles decorated multiwalled carbon nanotube**  
7  
8 **modified glassy carbon electrode**  
9

10  
11  
12 Mojtaba Kooshki, Hamid Abdollahi\*, Somayyeh Bozorgzadeh and Behzad Haghghi  
13  
14

15  
16  
17 Department of Chemistry, Institute for Advanced Studies in Basic Sciences, P.O. Box  
18  
19 45195 – 1159, Gava Zang, Zanjan, Iran. E-mail: [abd@iasbs.ac.ir](mailto:abd@iasbs.ac.ir) (H. Abdollahi); Tel.:  
20  
21 +98 241 415 3122; Fax: +98 241 415 3232.  
22  
23  
24  
25  
26  
27  
28  
29  
30  
31  
32  
33  
34  
35  
36  
37  
38  
39  
40  
41  
42  
43  
44  
45  
46  
47  
48  
49  
50  
51  
52  
53  
54  
55  
56  
57  
58  
59  
60  
61  
62  
63  
64  
65

**Abstract**

Three-way data obtained from different pulse heights of differential pulse voltammetry (DPV) was analyzed using multivariate curve resolution by alternating least squares (MCR-ALS) algorithm. Differential pulse voltammograms of tryptophan were recorded at a gold nanoparticles decorated multiwalled carbon nanotube modified glassy carbon electrode (GCE/MWCNTs-nanoAu). The determination of tryptophan was performed even in the presence of unexpected electroactive interference(s). Both the simulated and experimental data were non-bilinear. Therefore a Potential shift algorithm was used to correct the observed shift in the data. After correction, the data was augmented and MCR-ALS was applied to the augmented data. A relative error of prediction of less than 8% for the determination of the simulated analyte of interest and tryptophan in synthetic samples indicated that the methodology employing voltammetry and second-order calibration could be applied to complex analytical systems.

**Keywords:** Second order data, multivariate curve resolution by alternating least squares, Tryptophan, gold nanoparticles decorated multiwalled carbon nanotube modified glassy carbon electrode

## 1. Introduction

More than 30 years ago, Ernest R. Davidson and coworkers at the University of Washington published a five-page report [1] in which they introduced a new concept, second-order advantage, in analytical chemistry. This property, which can commonly be obtained from second-order data allows the quantification of the analyte(s) even in the presence of unexpected sample constituents [2]. Several approaches have been reported for obtaining second order data, such as fluorescence excitation–emission [3], HPLC–DAD [4], LC-ATR-FTIR [5], LC-DAD-MS [6], FIA-DAD [7], DAD-kinetics [8] and pH-DAD [9]. Although these approaches are highly accurate and reliable for the analysis, some of them suffer from several shortcomings such as the high cost of the instrumentation or the complexity of the instrumental method. Therefore, new methods are required for the inexpensive detection and quantification of analytes in a variety of matrices. Electrochemical methods provide good opportunities for accurate and reliable determination of analyte(s) using the low-cost instruments.

Electroanalytical data have been analyzed by many chemometricians during the past four decades. However, during the early development of these methods, the difficulty of the electrochemical hard modeling and the lack of linearity between the current and concentration restricted the application of chemometrics in electroanalytical chemistry [10]. Fortunately, the rapid development of artificial neural networks and dramatic improvements in soft modeling methods, have enhanced the application of chemometrics to electroanalytical data during the last several years [11]. Although several reviews have been published on the different aspects of the application of chemometrics in electroanalytical chemistry [12-16], in these reviews do not cover

1  
2  
3  
4 report of the electrochemical second-order advantage. Recently, two papers [17, 18]  
5  
6 have been published in this attractive field. In our previous work we reported the first  
7  
8 approach for producing electrochemical second-order data by changing an  
9  
10 instrumental parameter (pulse time in DPV). Because we used of an unmodified  
11  
12 carbon paste electrode, we could not determine low concentrations of the analyte of  
13  
14 interest. Another disadvantage of our previous work was the low sensitivity which  
15  
16 was also due to our use of an unmodified electrode [18]. These problems have  
17  
18 prompted us to use a sensitive sensor for quantifying the analyte of interest in the  
19  
20 present work.  
21  
22  
23  
24

25  
26 Tryptophan (Trp) is one of the essential amino acids which cannot be synthesized by the  
27  
28 organism. Therefore it must be supplied in the diet. This compound is a precursor for  
29  
30 serotonin (a neurotransmitter), melatonin (a neurohormone), and niacin. It has been  
31  
32 implicated as a possible cause of schizophrenia in people who cannot metabolize it  
33  
34 properly. The improper metabolization of Trp creates a toxic waste product in the brain  
35  
36 that causes hallucinations and delusions [19]  
37  
38  
39

40  
41 The direct electrochemical oxidation of Trp is known to be kinetically sluggish, and a  
42  
43 relatively high overpotential is required for its oxidation at bare electrodes[20].  
44  
45 Electrochemical detection of Trp has been shown to be facilitated by chemically modified  
46  
47 electrodes [20-22]. Substantial effort has been devoted to finding new mediators for the  
48  
49 fabrication of chemically modified electrodes that can decrease the overpotential of the  
50  
51 Trp oxidation. The oxidation peak potential for another electroactive amino acid, tyrosine  
52  
53 (Tyr), is very close to that of Trp. Consequently, Tyr is one of the usual interferences in  
54  
55  
56  
57  
58  
59  
60  
61  
62  
63  
64  
65

1  
2  
3  
4 the determination of Trp [23, 24]. Therefore, interest in the development of simple and  
5  
6 interference-free methods for the determination of Trp continues.  
7

8  
9 Nano-structured electrodes, including single electrodes on the nanometer scale and  
10  
11 electrodes composed of nano-materials represent new classes of electrodes that can  
12  
13 improve the performance of electroanalytical methods [25, 26]. Nano-structured  
14  
15 electrodes, in comparison to their bulk counterparts, provide a high effective surface area,  
16  
17 enhance mass transport, interact with some biological species efficiently and facilitate  
18  
19 their charge transfer. The attachment of metal nanoparticles (NPs) to carbon nanotubes  
20  
21 (CNTs), which is often referred as a “decoration” process may lead to the creation of new  
22  
23 nano-hybrid materials with the integrated properties of the two components [27]. In  
24  
25 addition, these nano-hybrid materials often show interesting properties that are not  
26  
27 exhibited by the respective components alone. Therefore, nano-hybrid materials can offer  
28  
29 opportunities for the development of new sensors and biosensors with high analytical  
30  
31 performance [27].  
32  
33  
34  
35  
36  
37

38 In the present work, as a part of our research on the applications of chemometrics to the  
39  
40 analysis of electrochemical data [18, 28] , we report a simple method based on changes in  
41  
42 the pulse height of DPV to create electrochemical second-order data. Because of the non-  
43  
44 bilinear behavior of the obtained data, the potential shift correction method is used for the  
45  
46 correction of the observed shifts in the data. Then, MCR-ALS is applied on the corrected  
47  
48 data to determine the concentration of the analyte. In the present work, a mixture of Trp  
49  
50 and Tyr has been chosen as a model for indicating the capability of the method.  
51  
52  
53  
54  
55  
56  
57  
58  
59  
60  
61

1  
2  
3  
4 Finally, the method is employed for the analysis of the electrochemical responses of the  
5  
6 new sensor for Trp determination at the gold nanoparticles decorated multiwalled carbon  
7  
8 nanotube modified glassy carbon electrode for the determination of Trp in meat extract.  
9

## 10 11 **2. Experimental**

### 12 13 **2.1. Reagents and chemicals**

14  
15 All chemicals were analytical reagent grade and used without further purification.  
16  
17 Gold(III) acetate (99.99%) was purchased from Alfa Aesar (Karlsruhe, Germany).  
18  
19 Sodium hydroxide, tryptophan, tyrosine and dimethylformamide (DMF) were obtained  
20  
21 from Merck (Darmstadt, Germany). Multiwalled carbon nanotubes (MWCNTs, 95%  
22  
23 purity, OD = 10-30 nm, ID = 5-10 nm and length = 0.5-500  $\mu\text{m}$ ) were obtained from  
24  
25 Aldrich (Steinheim, Germany). Double-distilled water was used throughout the  
26  
27 experiments..  
28  
29  
30  
31  
32

### 33 34 **2.2. Apparatus and software**

35  
36 DPV and cyclic voltammetry (CV) were performed using a Metrohm 746/747 VA and  
37  
38 an Autolab potentiostat-galvanostat, model PGSTAT30 (Utrecht, The Netherlands),  
39  
40 respectively with a conventional three-electrode set-up. A GCE/MWCNTs-nanoAu, an  
41  
42 Ag|AgCl|KCl<sub>sat</sub> electrode and a platinum wire served as the working, reference and  
43  
44 auxiliary electrodes, respectively. Scanning electron microscopy (SEM) was performed  
45  
46 with a Philips instrument; model XL-30 (Eindhoven, The Netherlands). A Metrohm 691  
47  
48 pH meter was used for pH measurements. All measurements were performed at room  
49  
50 temperature.  
51  
52

53  
54  
55 Voltammetric data were analyzed in the Matlab environment. MCR-ALS was  
56  
57 implemented using the graphical interface provided by Tauler in his web page[29].  
58  
59  
60  
61



### 2.3. Fabrication of GCE/MWCNTs-nanoAu

Au nanoparticles decorated MWCNTs were prepared according to the previously reported method [27]. In brief, the treatment of MWCNTs were treated by refluxing with 70% HNO<sub>3</sub> for 16 h, followed by the filtration and thorough washing of the material with deionized water until pH~7. The acid-treated MWCNTs were dried in a vacuum oven. The pretreated MWCNTs (8 mmol carbon equivalent) were dry mixed with powdered Au(CH<sub>3</sub>COO)<sub>3</sub> (0.08 mmol) using a mortar and pestle for about 30 min under ambient conditions to prepare AuNPs decorated MWCNTs with a 1 mol % Au loading. The solid, homogenous mixture of Au(CH<sub>3</sub>COO)<sub>3</sub> and MWCNTs was then transferred to a glass vial, heated under nitrogen in an oven to 300 °C for 1 h and isothermed for 3 h. The product was then collected as the AuNPs decorated MWCNTs (MWCNTs-nanoAu).

The surface of a glassy carbon electrode (GCE) was polished successively with 0.3 and 0.1 μm alumina paste (Struers, Copenhagen, Denmark) to a mirror finish and then cleaned in water under ultrasonication. One milligram of MWCNTs-nanoAu was dispersed in 1 ml DMF with ultrasonic agitation for 1 h to achieve a well-dispersed suspension. Then 2 μL of the prepared MWCNTs-nanoAu suspension was cast onto the surface of the GCE and dried in an oven at 50 °C to prepare a GCE modified with AuNPs decorated MWCNTs (GCE/MWCNTs-nanoAu).

### 2.4. Preparation of a real sample

A real sample was prepared according to previous reports [30]. The meat sample (250 mg) was dissolved in 3 mL of 4 M sodium hydroxide, sealed in a hydrolysis tube under nitrogen and incubated in an oven at 100 °C for 3 h. The mixture was cooled on an ice bath and neutralized to approximately pH 7 using concentrated HCl. The solution was

then diluted to 5 mL with 0.1 M phosphate buffer (pH 7.4). The final solution was filtered through a 0.45  $\mu\text{m}$  filter before the analysis.

### 3. Results and discussion

#### 3.1. Simulation of non-bilinear second-order data

As previously mentioned, the purpose of this work is to obtain second-order data via a simple change in one of the instrumental parameters of differential pulse voltammetry. In our previous work [18], we demonstrated that a change of the pulse duration(T) in DPV produced a bilinear simulated electrochemical data matrix for an electroactive species. In this work, the pulse height ( $\Delta E$ ) in DPV is changed to obtain electrochemical second-order data. The theory behind the proposed procedure will be briefly discussed.

The current signal intensity in differential pulse voltammetry for a reversible electrochemical reaction can be obtained using equation 1 [31],

$$\delta i = \frac{nFAD_o^{1/2}C_o^*}{\pi^{1/2}(\tau - \tau')^{1/2}} \left[ \frac{P_A(1 - \sigma^2)}{(\sigma + P_A)(1 + P_A\sigma)} \right] \quad (1)$$

where

$$P_A = \xi \exp \left[ \frac{nF}{RT} \left( E + \frac{\Delta E}{2} - E^{0'} \right) \right] \quad (2)$$

$$\sigma = \exp \left( \frac{nF}{RT} \frac{\Delta E}{2} \right) \quad (3)$$

$\xi = (D_O/D_R)^{1/2}$ ,  $\Delta E$  is the pulse height and other symbols have their conventional meanings.

For a typical electrochemical reaction, a data vector can be obtained by sweeping the

1  
2  
3  
4 potential at constant  $\Delta E$  and  $\tau$ . Applying a different  $\Delta E$  and sweeping potential at the  
5  
6 constant  $\tau$ , will produce different data vectors, i.e., sweeping the potential and  
7  
8 applying different pulse heights ( $\Delta E$ s) at a constant pulse duration in DPV produces a  
9  
10 non-bilinear second-order data. Then, because of the additive character of the current  
11  
12 signal, the second-order data of a two-component mixture can be obtained by adding  
13  
14 the current signals of the two components.  
15  
16

17  
18 For the simulation of a single-component mixture, we supposed that  $n = 2$ ,  $F = 96845$   
19  
20  $C$ ,  $A = 0.2 \text{ cm}^2$ ,  $D_{o1} = 5 \times 10^{-6} \text{ cm}^2 \text{ s}^{-1}$ ,  $C^*_{o1} = 4 \times 10^{-5} \text{ M}$ ,  $R = 8.314 \text{ J mol}^{-1} \text{ K}^{-1}$ ,  $T = 298 \text{ K}$ ,  
21  
22  $E_{o1} = 0.380 \text{ V}$ ,  $\tau = 20 \text{ ms}$  and  $\Delta E$  varies from 20 to 120 mV with a 20 mV increment.  
23  
24 For the simulation of a two-component mixture, we simulated the signal matrix of the  
25  
26 second species by supposing that  $D_{o2} = 6 \times 10^{-6} \text{ cm}^2 \text{ s}^{-1}$ ,  $C^*_{o2} = 1.5 \times 10^{-4} \text{ M}$ ,  $E_{o2} = 0.430$   
27  
28  $\text{V}$  and other parameters were assumed to be similar to those were used for the first  
29  
30 component. Previous reports on the simulation of DPV have confirmed the obtained  
31  
32 simulated data [32, 33].  
33  
34  
35  
36  
37

### 38 **3.2. Analysis of the simulated data**

#### 39 **3.2.1. Shift correction**

40  
41 Simulations for a typical reversible system were performed using the supposed values  
42  
43 mentioned previously (Fig.1). As it can be seen in the figure 1 by changing the pulse  
44  
45 height, the obtained simulated voltammograms shifted and broadened. Shift in peak  
46  
47 position for the electrochemically reversible systems happens with changing the pulse  
48  
49 height [31]. Similar to that was observed for the simulated data.  
50  
51  
52  
53

54  
55 A single analyte was considered to be present in the calibration samples of the  
56  
57 simulated system ( $S_1$ ,  $S_2$  and  $S_3$ ), whereas the interference was included in the test  
58  
59  
60  
61

1  
2  
3  
4 samples (M).  
5  
6  
7

8  
9 [Figure 1 should be here]  
10

11 When the obtained data is non-bilinear, the concentration of the analyte of interest  
12 can be estimated by non-bilinear rank annihilation (NBRA) [34, 35]. Because of the  
13 existence of non-bilinearity in this type of data, a pure component has a rank greater  
14 than one. It has been shown that NBRA yields multiple concentration estimates for  
15 the analyte of interest. These multiple estimates are usually not identical; some are  
16 correct, whereas others are not. Therefore, a concentration estimation of the analyte of  
17 interest is confusing. Borgen et al. developed a NBRA method for solving this  
18 problem by defining of some concepts such as net analyte rank (NAR) and rank linear  
19 additivity (RLA) [36]. Because, the obtained data in this work is full rank, application  
20 of Borgen's method for estimation of the analyte of interest seems to be impossible.  
21 We therefore, examined other methods for estimating the concentration of the analyte  
22 of interest.  
23  
24  
25  
26  
27  
28  
29  
30  
31  
32  
33  
34  
35  
36  
37  
38  
39

40 MCR-ALS as a powerful chemometrical method and, because it is a good candidate  
41 for solving aforementioned problem, was applied on a column-wise augmented data  
42 matrix obtained from three standards and one synthetic mixture sample. For the  
43 synthetic mixture containing the analyte of interest and the interference, satisfactory  
44 results were not obtained by MCR-ALS. The applied constraints in ALS were non-  
45 negativity, unimodality (for voltammogram profiles), equality constraint (for the  
46 voltammogram profile of the analyte) and selectivity. The lack of linearity in the  
47 system produced an excessive lack of fit (lof) of 30%, i.e., convergence was not  
48  
49  
50  
51  
52  
53  
54  
55  
56  
57  
58  
59  
60  
61

1  
2  
3  
4 achieved and the results of MCR-ALS were not satisfactory. The inefficiency of the  
5  
6 MCR-ALS model could be due to the potential shift of the data. The shift of potential  
7  
8 in the data as a possible source of inefficiency was therefore corrected as described  
9  
10 below.

11  
12  
13  
14 The main premise of multivariate curve resolution (MCR) techniques is to follow the  
15  
16 multicomponent Beer's law. Consequently, they can be used to analyze the bilinear data.  
17  
18 Applying chemometrics tools such as MCR-ALS to resolve data requires the uniform  
19  
20 presentation of data, i.e., all signals have to be adjusted to the same length and  
21  
22 corresponding variables have to be placed into the proper columns of the data matrix. The  
23  
24 signals obtained from voltammetric techniques often do not fulfill this requirement. This  
25  
26 problem is seen as the potential shift in electrochemical data. These facts cause a  
27  
28 decrease in the linearity, which depends on the magnitude of the potential shift. In many  
29  
30 cases, large *lof* values as the results of potential shift for MCR-ALS analysis are obtained  
31  
32 and impel the analyst to use a higher number of components to explain the non-linearity.  
33  
34 Diaz-Cruz et al. recently reported an approach to deal with this problem [10]. They  
35  
36 proposed an iterative algorithm in which all the voltammograms were aligned to the same  
37  
38 reference position. To correct the potential shift, they used three *Matlab* functions  
39  
40 including *peakmaker*, *shiftcalc* and *shiftfit*. *Peakmaker* is a function that generates a  
41  
42 Gaussian peak as an initial estimation of the pure voltammograms. The *shiftcalc* function  
43  
44 displaces every signal in every experimental voltammograms matrix for a given potential  
45  
46 shift  $\Delta E$ . The *shiftfit* function iteratively optimizes the values of  $\Delta E$  to generate a matrix  
47  
48 ( $\mathbf{I}_{cor}$ ) in which all signals remain at the fixed potentials stated in the pure voltammograms  
49  
50 matrix ( $\mathbf{V}_o$ ) matrix. To perform the potential shift correction, a matrix of the pure  
51  
52  
53  
54  
55  
56  
57  
58  
59  
60  
61  
62  
63  
64  
65

1  
2  
3  
4 voltammograms of the involved electroactive components is required. The pure  
5  
6  
7 voltammograms matrix ( $V_o$ ) was obtained from the simulated data matrix and the  
8  
9 *peakmaker* function. The pure voltammogram of the analyte of interest was obtained  
10  
11 from the simulated voltammograms of the standard solution of the analyte, and the pure  
12  
13 voltammogram of the interference was obtained using the non-bilinear data of the  
14  
15 mixture and the *peakmaker* function. Then, the mentioned pure voltammograms were  
16  
17 arranged in a matrix to create the pure voltammograms matrix ( $V_o$ ).  
18  
19

20  
21 The potential shift correction was performed on a column-wise augmented data  
22  
23 matrix that contained three standards of the simulated data matrices of the analyte of  
24  
25 interest. All voltammograms of the augmented data were investigated as the pure  
26  
27 voltammogram of analyte of interest in the *shiftfit* program. Then, the voltammogram  
28  
29 which produced the lowest error in potential shift correction was selected as the pure  
30  
31 voltammogram of the analyte of interest. The potential shift correction was also  
32  
33 performed on the synthetic mixture (M).  
34  
35  
36

37  
38 Although the potential shift correction can overcome the non-bilinearity in the data, it  
39  
40 produces rank deficient data for the synthetic mixture (M). The synthetic mixture  
41  
42 contained two components but the rank of the potential-shift-corrected synthetic  
43  
44 matrix was one. Significant results were not achieved for the resolution of this  
45  
46 corrected matrix by MCR-ALS. We therefore tried to overcome the rank deficiency  
47  
48 problem using matrix augmentation.  
49  
50  
51

### 52 53 54 55 **3.2.2. Breaking the rank deficiency of corrected data**

56  
57 Matrix augmentation has been reported as a simple and effective approach to the rank  
58  
59  
60  
61

1  
2  
3  
4 deficiency problem [37]. The strategy employed in this work is to augment the rank-  
5  
6 deficient signal matrix of the mixture with the potential-shift-corrected data matrices  
7  
8 of the standards of the simulated analyte.  
9

10  
11 Applying MCR-ALS on the augmented data produced a lof of approximately 7%,  
12  
13 which was better than that obtained without the potential shift correction. Figure 2  
14  
15 shows the potential shift correction of the augmented data for three simulated  
16  
17 standard solutions of the analyte of interest (top left), and one of the synthetic  
18  
19 mixtures, M (top right), which have been simulated at a pulse height of 20 to 100 mv  
20  
21 with a 20 mv interval. These corrected data were then augmented and standard MCR-  
22  
23 ALS was performed on the new augmented data. The results of the potential shift  
24  
25 correction and MCR-ALS analysis for the determination of the analyte of interest in  
26  
27 the synthetic mixtures (M) are given in Table 1. As evident from the data in the Table,  
28  
29 the analysis of the simulated data matrices performed by application of the potential  
30  
31 shift correction generates convergence with a much better fit and low lof values. As  
32  
33 shown in Table 1, the relative errors of prediction are acceptable; consequently, the  
34  
35 proposed method could be efficiently applied for the determination of the analyte in  
36  
37 the experimental data.  
38  
39  
40  
41  
42  
43  
44

45 [Figure 2 should be here]  
46  
47  
48  
49

### 50 51 **3.3. Characterization of GCE/MWCNTs-nanoAu**

52  
53 As shown in figure 1s in supplementary file, the SEM image of MWCNTs-nanoAu  
54  
55 powder revealed the formation of Au nanoparticles with diameters of approximately 60  
56  
57 nm on the walls of the carbon nanotubes.  
58  
59  
60  
61

1  
2  
3  
4 Figure 2s shows the cyclic voltammograms of a GCE (a), GCE/MWCNTs(b) and  
5  
6 GCE/MWCNTs-nanoAu(c) were recorded in 0.5 M H<sub>2</sub>SO<sub>4</sub> solution at a scan rate of 100  
7  
8 mV s<sup>-1</sup>. The CV of the GCE/MWCNTs-nanoAu showed a typical increase in the anodic  
9  
10 peak due to the oxidation of the gold surface on the forward scan (starting at  
11  
12 approximately 1.2 V) and its reduction on the reverse scan (at approximately 0.9 V). In  
13  
14 addition, the appearance of a pair of oxidation-reduction peaks at approximately 0.4 V is  
15  
16 attributed to the quasi-reversible electrochemical behavior of quinone-type carbon  
17  
18 oxygen functionalities on the surface of acid-treated MWCNTs, [38] .  
19  
20  
21  
22

### 23 **3.3.1. Voltammetric characteristics of Trp on GCE/MWCNTs-nanoAu**

24 Preliminary experiments were performed to characterize the behavior of Trp at  
25  
26 GCE/MWCNTs-nanoAu. Figure 3 shows the differential pulse voltammograms  
27  
28 obtained at GCE (a) in phosphate buffer at pH 7.4 without Trp, and at GCE (b),  
29  
30 GCE/MWCNTs (c) and GCE/MWCNTs-nanoAu(d) in the presence of 100 μM Trp.  
31  
32 As evident in Fig. 3, the peak potentials of oxidation of Trp at GCE/MWCNTs and  
33  
34 GCE/MWCNTs-nanoAu, in comparison with that of GCE, shift approximately 80 and  
35  
36 180 mV, respectively, in the negative direction. In contrast, the peak current of Trp  
37  
38 significantly increases after the AuNPs have been decorated on the MWCNTs surface,  
39  
40 which indicates the excellent electrocatalytic activity of the MWCNTs-nanoAu hybrid  
41  
42 toward Trp oxidation.  
43  
44  
45  
46  
47  
48  
49

50 [Figure 3 should be here]  
51  
52  
53  
54

### 55 **3.3.2. Effect of experimental variables on the anodic peak current of Trp**

56 In the present work, a mixture of Trp and Tyr was chosen as a model mixture to  
57  
58  
59  
60  
61



1  
2  
3  
4 demonstrate the ability of the proposed method. Trp was chosen as the analyte of  
5  
6 interest and Tyr was selected as a typical interference in the Trp determination. To  
7  
8 select the best conditions for the determination of Trp, the effect of the experimental  
9  
10 variables on the peak current of the anodic differential pulse voltammograms of Trp  
11  
12 were investigated.  
13  
14

15  
16 Figure 4A shows the influence of the pH of the Britton-Robinson solution, in the  
17  
18 range of 2 to 9, on the current signal intensities of 100  $\mu\text{M}$  Trp. The peak currents did  
19  
20 not change significantly up to a pH of 7.4 but decreased significantly at higher pH  
21  
22 levels. Thus, a pH of 7.4 for the physiologic buffer was adopted for further studies.  
23  
24

25  
26 The anodic peak potential of the Trp shifted to more negative values as the pH of the  
27  
28 buffer solution was increased (Fig. 4B). The negative shift in the anodic peak potential  
29  
30 with increasing pH showed a linear behavior with a slope of  $-49.9 \text{ mV pH}^{-1}$  and an  $R^2$  of  
31  
32 0.9991. This result reveals that the number of protons in the electrochemical reaction is  
33  
34 equal to the number of transferred electrons.  
35  
36

37  
38 The effect of the loading of MWCNTs-nanoAu on the anodic peak current intensity was  
39  
40 evaluated by casting different amounts of MWCNTs-nanoAu suspension on the GCE  
41  
42 surface (not shown). The amount of MWCNTs-nanoAu on the surface of the electrode is  
43  
44 clearly a dominant factor for the oxidation of Trp and for the peak current. The peak  
45  
46 current was enhanced by an increase in the amount of MWCNTs-nanoAu and reached a  
47  
48 plateau when 2  $\mu\text{L}$  of MWCNTs-nanoAu ( $1 \text{ mg mL}^{-1}$ ) was cast. Thus, 2  $\mu\text{L}$  of  
49  
50 MWCNTs-nanoAu ( $1 \text{ mg mL}^{-1}$ ) was selected for the sensor fabrication.  
51  
52  
53  
54  
55  
56

57  
58 [Figure 4 should be here]  
59  
60  
61

1  
2  
3  
4  
5  
6  
7 Figure 5 shows the anodic differential pulse voltammograms of Trp (a), Tyr (b) and a  
8  
9 mixture of Trp and Tyr (c) at the GCE/MWCNTs-nanoAu under the optimized  
10  
11 conditions. As mentioned in the introduction, and as can be observed in Figure 5, the  
12  
13 voltammograms of Trp and Tyr exhibit severe overlapping.  
14  
15

16  
17  
18  
19 [Figure 5 should be here]  
20  
21  
22

### 23 **3.4. Application of the proposed method for the experimental data**

24  
25  
26 M CR-ALS was performed on a column-wise augmented data matrix obtained from  
27  
28 the DPV results of the three standards and a synthetic mixture sample solution. For  
29  
30 the synthetic mixture containing Trp and Tyr, satisfactory results were not obtained  
31  
32 by MCR-ALS. The applied constraints in ALS were similar to the simulation data.  
33  
34 The system's lack of linearity produced an excessive lof of 30%. As previously  
35  
36 mentioned, the results of MCR-ALS were not satisfactory because of the presence of  
37  
38 potential shifts in the experimental data. Therefore, the potential shift in the data was  
39  
40 corrected.  
41  
42  
43  
44

45  
46 Figure 6 shows the potential shift correction of the augmented data for three standard  
47  
48 Trp solutions (top left) and for a synthetic mixture solution containing 40  $\mu\text{M}$  Trp and  
49  
50 80  $\mu\text{M}$  Tyr (top right), which were obtained at a pulse height of 20 to 100 mV with a  
51  
52 20 mV interval. These corrected data were augmented, and MCR-ALS was performed  
53  
54 on them. The results of the potential shift correction and the MCR-ALS analysis for  
55  
56 the determination of Trp in the synthetic mixtures (M) are given in Table 2. As  
57  
58  
59  
60  
61

1  
2  
3  
4 indicated by the results in Table 2, the analysis of the synthetic data matrices that was  
5  
6 performed by application of the potential shift correction generates convergence with  
7  
8 a much better fit and low lof values.  
9

10  
11  
12  
13  
14  
15  
16 [Figure 6 should be here]  
17

### 18 **3.5. Figure of merit**

19  
20 After decomposition of data matrix by MCR-ALS, the concentration information  
21  
22 contained in the concentration profiles can be used for quantitative predictions in a  
23  
24 manner similar to that described in ref [9]. In that approach the area under the profile is  
25  
26 considered as proportional to component concentration, then the required pseudo-  
27  
28 univariate graph is built [9]. Then the figure of merit can be obtained by simple  
29  
30 calculations for univariate calibration. The sensitivity is the slope of calibration and limit  
31  
32 of detection can be calculated as  $3s/m$ .  
33  
34  
35  
36  
37

38 The calibration plot based on the area under concentration profiles was found to be linear  
39  
40 in the 5 – 100  $\mu\text{M}$  Trp ( $Y=.0271X + 0.8871$  with  $R^2=9993$ ). Limit of detection was 3  $\mu\text{M}$   
41  
42 of Trp.  
43  
44  
45  
46

### 47 **3.6. Real sample analysis**

48  
49 We assessed the analytical utility of the proposed method was assessed by applying it to the  
50  
51 determination of Trp in a fresh meat sample. 1 ml of meat sample extract was added to a  
52  
53 volumetric flask and diluted to the mark with the supporting electrolyte (0.1 M phosphate  
54  
55 buffer at pH 7.4). Differential pulse voltammograms for the prepared sample solution  
56  
57 were recorded (Fig 3s). The potential shift in the real sample data was corrected. The  
58  
59  
60  
61

1  
2  
3  
4 obtained matrix was augmented with the standards matrices, and then MCR-ALS was  
5  
6 performed. The results of the Trp determination in the real sample are summarized in  
7  
8 Table 3. For a meat extract the amount of Trp was reported in first row of Table 3. In  
9  
10 order to evaluate the accuracy of method three spiked samples (rows 3-5 in Table 3) were  
11  
12 prepared and recoveries in determination of Trp were calculated. The good recoveries  
13  
14 obtained for the spiked samples indicate the successful application of the proposed  
15  
16 method for the determination of Trp.  
17  
18  
19  
20  
21  
22

#### 23 **4. Conclusion**

24  
25  
26 The main goals of this work were (I) to create electrochemical second-order data and (II)  
27  
28 to perform the analysis in the presence of an unexpected interference. To achieve the first  
29  
30 goal, second-order data were created using a simple change in pulse height of differential  
31  
32 pulse voltammetry. Because of the non-bilinear behavior of the simulated and  
33  
34 experimental data, the potential shift correction algorithm and MCR-ALS were applied to  
35  
36 achieve the second goal. Additionally, a gold nanoparticle decorated multiwalled carbon  
37  
38 nanotube modified glassy carbon electrode was used as a sensitive sensor was used for  
39  
40 the determination of Trp. The proposed sensor exhibited an efficient electrocatalytic  
41  
42 activity toward Trp oxidation, which led to a decrease in the overpotential of the process  
43  
44 and a remarkable enhancement of the anodic peak current. The proposed method,  
45  
46 together with the proposed sensor, was successfully applied for the determination of Trp  
47  
48 in a meat sample with satisfactory results. This work proposed the use of a modified  
49  
50 electrode to overcome the low sensitivity and high limit of detection that we reported in  
51  
52 our previous work. These investigations are the starting point for the production of  
53  
54  
55  
56  
57  
58  
59  
60  
61  
62  
63  
64  
65

1  
2  
3  
4 electrochemical second-order data; future studies in this new field will involve the  
5  
6 development of more reliable sensors for electroanalytical determinations.  
7  
8  
9

## 10 11 12 **5. Acknowledgement** 13

14  
15 The authors acknowledge the Institute for Advanced Studies in Basic Science for  
16  
17 financial support (grant number G2011IASBS117). They are also grateful to Hassan  
18  
19 Hamidi for useful discussions.  
20  
21  
22  
23  
24  
25  
26  
27  
28  
29  
30  
31  
32  
33  
34  
35  
36  
37  
38  
39  
40  
41  
42  
43  
44  
45  
46  
47  
48  
49  
50  
51  
52  
53  
54  
55  
56  
57  
58  
59  
60  
61  
62  
63  
64  
65

**References**

- [1] C.N. Ho, G.D. Christian, E.R. Davidson, *Anal. Chem.*, 50 (1978) 1108-13.
- [2] K.S. Booksh, B.R. Kowalski, *Anal. Chem.*, 66 (1994) A782-A91.
- [3] T. Madrakian, A. Afkhami, M. Mohammadnejad, *Anal. Chim. Acta*, 645 (2009) 25-9.
- [4] Y. Zhang, H.L. Wu, A.L. Xia, Q.J. Han, H. Cui, R.Q. Yu, *Talanta*, 72 (2007) 926-31.
- [5] A. Edelmann, J. Diewok, J.R. Baena, B. Lendl, *Anal. Bioanal. Chem.*, 376 (2003) 92-7.
- [6] E. Pere-Trepat, R. Tauler, *J. Chromatogr. A*, 1131 (2006) 85-96.
- [7] A. Checa, R. Oliver, J. Saurina, S. Hernandez-Cassou, *Anal. Chim. Acta*, 572 (2006) 155-64.
- [8] M.J. Culzoni, P.C. Damiani, A. Garcia-Reiriz, H.C. Goicoechea, A.C. Olivieri, *Analyst*, 132 (2007) 654-63.
- [9] H.C. Goicoechea, A.C. Olivieri, *Appl.Spectrosc.*, 59 (2005) 926-33.
- [10] A. Alberich, J.M. Diaz-Cruz, C. Arino, M. Esteban, *Analyst*, 133 (2008) 112-25.
- [11] M. Esteban, C. Arino, J.M. Diaz-Cruz, *Crit. Rev. Anal. Chem.*, 36 (2006) 295-313.
- [12] S.D. Brown, R.S. Bear, *Crit. Rev. Anal. Chem.*, 24 (1993) 99-131.
- [13] Y.N. Ni, S. Kokot, *Anal. Chim. Acta*, 626 (2008) 130-46.
- [14] M. Esteban, C. Arino, J.M. Diaz-Cruz, *Trac-Trend. Anal. Chem.*, 25 (2006) 86-92.
- [15] V. Pravdova, M. Pravda, G.G. Guilbault, *Anal. Lett.*, 35 (2002) 2389-419.

- 1  
2  
3  
4 [16] E. Richards, C. Bessant, S. Saini, *Electroanalysis*, 14 (2002) 1533-42.  
5  
6  
7 [17] T. Galeano-Diaz, A. Guiberteau-Cabanillas, A. Espinosa-Mansilla, M.D. Lopez-  
8  
9 Soto, *Anal. Chim. Acta*, 618 (2008) 131-9.  
10  
11 [18] H. Abdollahi, M. Kooshki, *Electroanalysis*, 22 (2010) 2245-53.  
12  
13  
14 [19] W. Kochen, and H. Steinhart, *l-Tryptophan-Current Prospects in Medicine and*  
15 *Drug Safety*; de-Gruyter: Berlin, 1994.  
16 [20] S. Shahrokhian, L. Fotouhi, *Sensor. Actuators B: Chem.*, 123 (2007) 942-9.  
17  
18 [21] K.-J. Huang, C.-X. Xu, W.-Z. Xie, W. Wang, *Colloid. Surface. B* 74 (2009) 167-  
19  
20 71.  
21  
22 [22] Y. Guo, S. Guo, Y. Fang, S. Dong, *Electrochim. Acta*, 55 (2010) 3927-31.  
23  
24 [23] G.-P. Jin, X.-Q. Lin, *Electrochem. Commun.*, 6 (2004) 454-60.  
25  
26 [24] F.-H. Wu, G.-C. Zhao, X.-W. Wei, Z.-S. Yang, *Microchim. Acta*, 144 (2004) 243-  
27  
28 7.  
29  
30 [25] J.J. Gooding, *Electrochim. Acta*, 50 (2005) 3049-60.  
31  
32 [26] P. Bertonecello, R.J. Forster, *Biosens. Bioelectron.*, 24 (2009) 3191-200.  
33  
34 [27] Y. Lin, K.A. Watson, S. Ghose, J.G. Smith, T.V. Williams, R.E. Crooks, W. Cao,  
35  
36 J.W. Connell, . *J. Phys. Chem. C*, 113 (2009) 14858-62.  
37  
38 [28] E. Shams, H. Abdollahi, M. Yekehtaz, R. Hajian, *Talanta*, 63 (2004) 359-64.  
39  
40 [29] R. tauler, <http://www.ub.es/gesq/mcr/mcr.htm>.  
41  
42 [30] H. Schneider, N. Gerber, B. Friedli-Wunderli, C. Wenk, R. Amado, *Mitteilungen*  
43  
44 *aus Lebensmitteluntersuchung und Hygiene*, 97 (2006) 489-98.  
45  
46 [31] Faulkner.L.R. Bard. A. J, *Electrochemical Methods: fundamental and application*  
47  
48 *2<sup>nd</sup> ed.* Wiley New York, 2001.  
49  
50 [32] S.C. Rifkin, D.H. Evans, *Anal. Chem.*, 48 (1976) 2174-9.  
51  
52  
53  
54  
55  
56  
57  
58  
59  
60  
61  
62  
63  
64  
65

- 1  
2  
3  
4 [33] J.L. Melville, R.G. Compton, *Electroanalysis*, 13 (2001) 123-30.  
5  
6 [34] B.E. Wilson, B.R. Kowalski, *Anal. Chem.*, 61 (1989) 2277-84.  
7  
8  
9 [35] B.E. Wilson, W. Lindberg, B.R. Kowalski, *J. Am. Chem. Soc.*, 111 (1989) 3797-  
10 804.  
11  
12  
13 [36] Y.D. Wang, O.S. Borgen, B.R. Kowalski, M. Gu, F. Turecek, *J. Chemometr.*, 7  
14 (1993) 117-30.  
15  
16  
17 [37] A. Izquierdo Ridorsa, J. Saurina, S. HernandezCassou, R. Tauler, *Chemometr.*  
18 *Intell. Lab.*, 38 (1997) 183-96.  
19  
20  
21 [38] B. Haghghi, S. Bozorgzadeh, L. Gorton, *Sensor. Actuators B: Chem.*, 155  
22 (2011)577.  
23  
24  
25  
26  
27  
28  
29  
30  
31  
32  
33  
34  
35  
36  
37  
38  
39  
40  
41  
42  
43  
44  
45  
46  
47  
48  
49  
50  
51  
52  
53  
54  
55  
56  
57  
58  
59  
60  
61  
62  
63  
64  
65



1  
2  
3  
4  
5  
6  
7 **Figures captions:**  
8  
9

10 **Figure 1** Simulated DPV second-order data for a typical electroactive species by the  
11 proposed method. The pulse heights were 20 to 120 mv with a 20 mv  
12 interval  
13  
14  
15  
16

17 **Figure 2:** Application of potential shift correction, augmentation of the corrected data,  
18 and resolving of the augmented data by MCR-ALS for the simulated data of  
19 standards (top left) and the simulated data of a synthetic mixture (top right).  
20  
21  
22  
23  
24

25 **Figure 3:** Differential pulse voltammograms obtained at GCE (a) in phosphate buffer  
26 solution at pH 7.4 without Trp and at GCE (b), GCE/MWCNTs (c) and  
27 GCE/MWCNTs-nanoAu (d) in the presence of 100  $\mu\text{M}$  Trp.  
28  
29  
30  
31

32 **Figure 4:** A) Differential pulse voltammograms of 100  $\mu\text{M}$  Trp at a GCE/MWCNTs-  
33 nanoAu in Britton–Robinson buffer at different pH levels: a, b, c, d, e, f, g  
34 and h were recorded in buffers at pH levels of 1.97, 3.27, 4.02, 5.44, 6.46,  
35 7.35, 8.34 and 9.31, respectively. B) Plot of the peak potential variation with  
36 pH; the conditions are the same as in Fig. 4A.  
37  
38  
39  
40  
41  
42  
43

44 **Figure 5:** Differential pulse voltammograms obtained for a) a 50  $\mu\text{M}$  Trp solution b) a  
45 50  $\mu\text{M}$  Tyr solution and c) a synthetic mixture containing 50  $\mu\text{M}$  Trp and 50  
46  $\mu\text{M}$  Tyr under the optimized conditions.  
47  
48  
49  
50

51 **Figure 6:** Application of potential shift correction, augmentation of the corrected data,  
52 and resolution of the augmented data by MCR-ALS for the experimental  
53 data of standards (top left) and of a synthetic mixture (top right).  
54  
55  
56  
57  
58  
59  
60  
61

1  
2  
3  
4  
5  
6  
7  
8  
9  
10  
11  
12  
13  
14  
15  
16  
17  
18  
19  
20  
21  
22  
23  
24  
25  
26  
27  
28  
29  
30  
31  
32  
33  
34  
35  
36  
37  
38  
39  
40  
41  
42  
43  
44  
45  
46  
47  
48  
49  
50  
51  
52  
53  
54  
55  
56  
57  
58  
59  
60  
61  
62  
63  
64  
65

**Tables captions:**

Table 1. MCR-ALS analysis for the determination of the analyte of interest in the simulated unknown samples

Table 2. Results of the potential shift correction and MCR-ALS analysis in the Trp determination in the synthetic samples

Table 3. Results of the analysis of Trp in a real sample using the proposed method